

# Synthesis, Characterization, antimicrobial activity and Computational Study of New 3-(1-methyl-2-((1E,2E)-3-phenylallylidene)hydrazinyl)-5-phenyl-4H-1,2,4-triazole with some transition metal ions

Lina Abdulla Naser  
Nursing technology department  
/Southern Technical  
University/Nasiriyah Technical  
Institute  
Nasiriyah/Iraq  
[lina.abdullah@stu.edu.iq](mailto:lina.abdullah@stu.edu.iq)

Ali F. Nasir  
Directorate of Thi-Qar Education  
Nasiriyah/Iraq  
[Aliali1990@gmail.com](mailto:Aliali1990@gmail.com)

Zahraa M. Mahdi  
Department of Pharmacy/ Mazaya  
University College  
Nasiriyah/Iraq  
[zahraa.muhammed@mpu.edu.iq](mailto:zahraa.muhammed@mpu.edu.iq)

**Abstract**—Current study generated complexes of the novel heterocyclic ligand 3-(1-methyl-2-((1E,2E)-3-phenylallylidene)hydrazinyl)-5-phenyl-4H-1,2,4-triazole with Cr(III), Co(II), and Cu(II). Using techniques including <sup>1</sup>H-NMR, mass spectrometry, FT-IR, and elemental analysis, scientists could determine key characteristics of the novel ligand. As spectra, Fourier transforms infrared (FTIR), magnetic susceptibility, atomic absorption, and conductance measurements were used to describe ligand complexes in contrast. Bacteria were used in an assay to test the antibacterial activity of each novel compound (Staphylococcus and Escherichia coli). Quantum chemical simulations performed using the DFT approach at the B3LYP/6-311++G level complemented the experimental data. Using Hyperchem 8.02 and the PM3 approach, this study has determined the ligand's electrostatic potential and its complexes' geometries. The electrostatic potential that reveals useful data about the location's complexity.

**Keywords**—"ligand, complexes, characterization, antimicrobial, Triazoles, heterocyclic"

## I. INTRODUCTION

Triazoles are a group of heterocyclic compounds characterized by a 5-membered ring, 2 C, and 3 N atoms [1]. It is divisible into three isomers depending on where the nitrogen atom is located inside the ring: 1,2,3-triazole "vicinal triazole"; 1,2,4-triazole "asymmetrical-triazole"; 1,3,4-triazole "symmetrical-triazole" [2]. Antioxidant [3,4], anti-inflammatory [5,6], anticancer [6,7], antiviral [8,9], antifungal [10,11], antihypertensive, and antibacterial activities [3,4] are only a few of the pharmacologically significant traits displayed by 2,4-triazole. This is important, but it is not all: it has been shown that Schiff bases derived from triazole molecules also exhibit certain biological functions [11]. Coordination chemistry owes much of its history to Schiff base complexes with transition metals [12,13]. The commercial and biological uses of Schiff base metal complexes have led to their study [14-17].

## II. EXPERIMENTAL

The solvents and chemicals that have been utilized in this research, were all have the highest quality and purity levels commercially accessible. Chloride was substituted for all other metal salts.

### A. Physical Measurements

In an electrothermal melting point apparatus model "Melting SMP31", the melting point or the decomposition temperature of all the produced ligands and complexes of the transition metal were determined. A Shimadzu FTIR spectrophotometer with the model number "Model: IR-affinity, Shimadzu" was used to record the FTIR spectra as KBr disc for the ligand and CsI for the complexes. Bruker DXR System AL500 was used to obtain nuclear magnetic resonance spectra (500 MHz). Using the "Network Mass Selective Detector 5973," mass spectra were collected.

### B. Preparation of the ligand"

#### 1. "Synthesis of benzohydrazide"

Methyl benzoate (30.4ml, 0.2mol) and hydrazine monohydrate (15.0ml, 0.3mol) were combined with 30ml of ethanol absolute, refluxed for 6 hours, evaporated to half volume, cooled, filtered(qualitative filter paper), and then washed with more ethanol absolute. The solid (A) had a melting point of 114–115°C and a 97% yield.

#### 2. The Synthesis of 1-benzoyl-thiosemicarbazide"

Potassium thiocyanate (19.4 g, 0.2 mol), benzohydrazide (1) (26 g, 0.2 mol), and 40 mL of concentrated HCl were refluxed in 100 mL of ethanol for four hours. After cooling, a white solid emerged that was filtered and dried. m.p. 199-201°C; yield (71%). 3280 (NH), 1670 (CONH), and 1360 (C=S) in IR (KBr, cm<sup>-1</sup>)

#### 3. "The Synthesis of 5-phenyl-4H-1,2,4-triazole-3-thiol"

In 40.00 ml of ethanol, 19.5 g of 1-benzoyl-thiosemicarbazide and 5.6 g of potassium hydroxide were refluxed for four hours before cooling and filtering. The

clear solution was then brought to a pH of 5–6 by adding concentrated HCl. White crystals were produced by filtering and recrystallizing the solid (methanol). IR (KBr,  $\text{cm}^{-1}$ ): 2575 (SH), 1605 (C=N), and 1325 (C=S); Yield (80%), m.p. > 250°C.

#### 4. Synthesis of 3-hydrazinyl-5-phenyl-4H-1,2,4-triazole

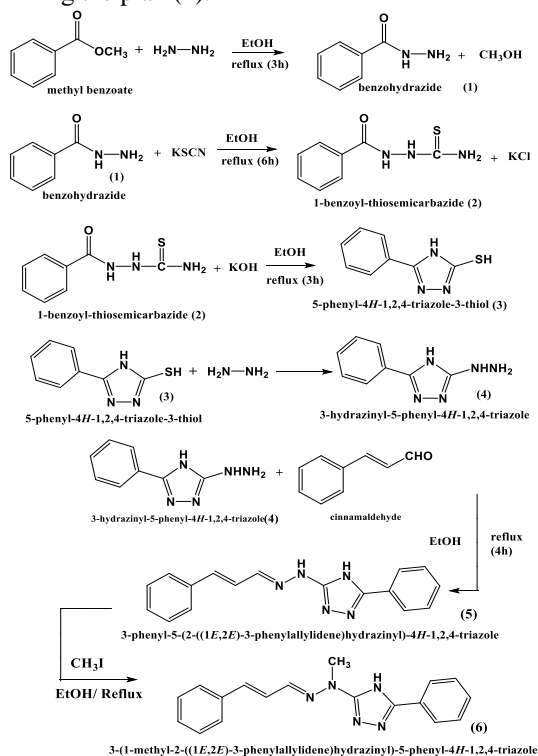
For 16 hours, ethanol absolute (40 ml) was used as the solvent for 5-phenyl-4H-1,2,4-triazole-3-thiol (17.7 g, 0.1mol) and hydrazine monohydrate (5 ml, 0.1mol). When the white precipitate formed in the circular bottom, the ethanol absolute was filtered and recrystallized. yield 62%, melting point (180-220)°C.

#### 5. 3-(1-phenyl-5-(2-((1E,2E)-3-phenylallylidene)hydrazinyl)-4H-1,2,4-triazole"

Synthesis of the Schiff base included the condensation in 100% ethanol of 3-hydrazinyl-5-phenyl-4H-1,2,4-triazole (17.5 g, 0.1 mol) and cinnamaldehyde (13.2 g, 0.1 mol) (40ml). The reaction mixture was then allowed to reflux for 8 hours while being monitored by TLC (Thin – layer chromatography), after which the ligand was precipitated, filtered, and recrystallized from ethanol absolute to produce a yellow ligand with a melting point of 228-230°C and a yield of 78%.

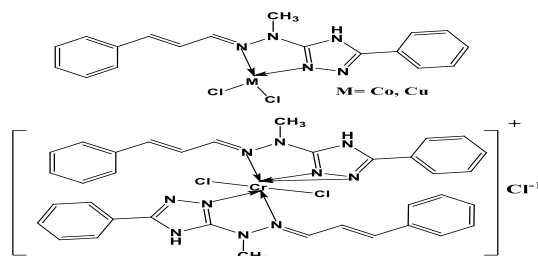
#### 6. 3-(1-methyl-2-((1E,2E)-3-phenylallylidene)hydrazinyl)-5-phenyl-4H-1,2,4-triazole

Synthesis of the ligand included the condensation of 3-phenyl-5-(2-((1E,2E)-3-phenylallylidene)hydrazinyl)-4H-1,2,4-triazole (14.5 g, 0.05 mol) and methyl iodide (7.1 g, 0.05 mol) in pure ethanol (50ml). Finally, after 7 hours of refluxing (under TLC observation), the ligand was precipitated, filtered, and recrystallized from 100% ethanol to provide a melting point of 239-241°C and a yield of 68%. following the plan (1).



### C. Preparation of complexe

The complexes were produced by refluxing a solution containing 0.001mol of ligand and the salts "CrCl<sub>3</sub>.6H<sub>2</sub>O, and CoCl<sub>2</sub>.6H<sub>2</sub>O, CuCl<sub>2</sub>.H<sub>2</sub>O i (15ml) ethanol absolute while being monitored by TLC for 2 hours. After numerous washes in ethanol or aqueous ethanol to eliminate unreacted salts or ligands, the precipitate was filtered, and the resulting complexes were dried.



## III. RESULT AND DISCUSSION"

### A. "Synthesis of ligand L"

Scheme 1 outlines the synthetic approach taken to create the ligand L. Methyl benzoate was used as the starting material for all four processes (1-4) required to produce the crucial intermediate 4.

### B. Analysis and physical measurements

Tables 1 and 2 display the molecular formula, melting point, and elemental analyses (CHNS) of the produced derivatives of 1,2,4-triazole-bearing Schiff base (1). mass spectra, 1HNMR, FT-IR, and CHNS elemental studies are used to determine the structural formula. The resulting findings correlate well with those estimated using the proposed formula.

### C. "FT-IR spectra

The KBr disc was used to analyze the ligand and the CsI to analyze the complexes using FT-IR. At (3111), (3072), (1627), (1585), (1546), (1365) and (1274), the free ligand (L) has shown prominent bands. As indicated in table (2) and figure below, these frequencies correspond to the ( $\nu$ N-H), ( $\nu$ C-H)aro, ( $\nu$ C=N)oxo, ( $\nu$ C=N)endo, ( $\nu$ C=C), ( $\nu$ C=N)asym, and ( $\nu$ C-N-C) sym bands (9). It was found that new bands emerged in the spectra of complexes. Coordinated (M-N) and ( $\nu$ M-Cl) bonds were responsible for the appearance of these modes of vibration in the (528-620)  $\text{cm}^{-1}$  and (223-266)  $\text{cm}^{-1}$  regions, respectively. This proves that a stable five-member ring was formed via a coordinate transformation involving the (N) and (Cl) atoms.

### D. "Nuclear Magnetic Resonance"

The <sup>1</sup>HNMR spectra of the ligand has shown signals at "2.51 and 3.27 ppm", the first due to protons of the solvent (DMSO) and the second for the water, (3.87 ppm, s, 3H) due to the proton of CH<sub>3</sub> group, "7.10 ppm, dd, J=15 Hz, J=10 Hz, 1H" due to the proton of C=CH, "7.26 ppm, d, J=15 Hz, 1H" due to the proton of HC=C, (7.19-7.93 ppm, m, 8H) due to protons of aromatic rings, "8.37 ppm, d, J=10 Hz, 1H" due to the proton of azo methane group (-N=CH), (13.73 ppm, s, 1H) due to N-H proton in the triazole ring [18], as shown in figure (11).

Table (1) ligand and complex physical characteristics, elemental microanalysis (CHN), metal proportion

NO	Formula	color	"C %"	"H %"	"N %"	"M%"	" $\Lambda$ scm <sup>2</sup> mol <sup>-1</sup> "	"M.p °C"	" $\mu$ eff.B.M"
1	C <sub>18</sub> H <sub>17</sub> N <sub>5</sub> (L)	White	69.34exp. 71.27cal.	6.29exp. 5.65cal.	24.96exp 23.09cal	.....	.....	239-241	.....
2	[Cr(L) <sub>2</sub> Cl <sub>2</sub> ]Cl	green yellowish	.....	.....	.....	7.94	36.65	248-250	3.8
3	[Co(L)Cl <sub>2</sub> ]	brown	.....	.....	.....	15.16	15.47	257-259	4.1
4	[Cu(L)Cl <sub>2</sub> ]	Green	.....	.....	.....	16.73	8.73	262-264	1.9

#### E. "Mass spectra"

There was a molecular ion peak at 304 m/z in the mass spectra of the ligand, which agrees with the molecular formula C<sub>18</sub>H<sub>17</sub>N<sub>5</sub>. Those succeeding pieces account for the other peaks, which include [C<sub>17</sub>H<sub>14</sub>N<sub>5</sub>]<sup>+</sup>=288 m/z, [C<sub>12</sub>H<sub>12</sub>N<sub>5</sub>]<sup>+</sup>=226 m/z, [C<sub>10</sub>H<sub>10</sub>N<sub>5</sub>]<sup>+</sup>=200 m/z, [C<sub>9</sub>H<sub>9</sub>N<sub>4</sub>]<sup>+</sup>=173 m/z, [C<sub>12</sub>H<sub>12</sub>N<sub>3</sub>]<sup>+</sup>=226 m/z, [C<sub>10</sub>H<sub>11</sub>N<sub>2</sub>]<sup>+</sup>=159 m/z, [C<sub>9</sub>H<sub>8</sub>N]<sup>+</sup>=130 m/z, [C<sub>8</sub>H<sub>7</sub>]<sup>+</sup>=103 m/z, [C<sub>8</sub>H<sub>6</sub>N<sub>3</sub>]<sup>+</sup>=145 m/z, [C<sub>6</sub>H<sub>5</sub>]<sup>+</sup>=77 m/z, [CH<sub>3</sub>N<sub>3</sub>]<sup>+</sup>=57 m/z base peak.

Molecular ion peaks at 765 m/z were seen in the mass spectrum of Cr (III) complexes, which are consistent with the [Cr(L)<sub>2</sub>Cl<sub>2</sub>]Cl<sup>+</sup> stoichiometry. Another fragmentation peak at 730 m/z, followed by peaks at 694 and 659 owing to the loss of three chlorine atoms, are seen for this complex. Molecular ion peaks at 4333 m/z, corresponding to [Co(L)Cl<sub>2</sub>], were seen in the mass spectra of Co (II) complexes. the stoichiometry plus sign. In addition to the peak at 397 m/z, this compound also exhibits a peak at 362 m/z, indicating the loss of two chlorine atoms. Mass spectroscopy of Cu (II) complexes revealed molecular ion peaks around 438 m/z, which are consistent with the stoichiometry [Cu (L)Cl<sub>2</sub>]<sup>+</sup>. The loss of two chlorine atoms from this complex produces a second fragmentation peak at 402 m/z and a third at 367 m/z.

#### F. Magnetic susceptibility

The magnetic momentum for each metal complex is listed in table (1). These magnetic measurements give information about the electronic state the transition talme ions of the complexes. The observed magnetic momentum value of the Cr(III) complex was 3.8 BM, which is expected to be an octahedral geometry, Co(II) is 4.1 BM implying a tetrahedral geometry, andy, Cu(II) is 1.9 BM implying square laner geometry<sup>[19]</sup>.

#### G. "Molar conductivity measurements"

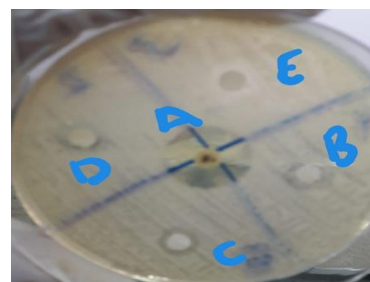
At room temperature, in DMSO as a solvent with a concentration of 1×10<sup>-3</sup> M, the molar conductivity of the prepared material complex was measured. The conductivity values are listed in Table (1). The molar conductivity of the Cr(III) complex shows that the complex is a 1:2 (metal: ligand) electrolyte with ionic properties, and this is proved by using a silver nitrate (AgNO<sub>3</sub>) solution in which silver chloride is formed. The white precipitate (AgCl). Although it shows lower molar conductivity values of Co(II) and Cu(II) complexes, it indicates that these complexes have anon-ionic structure and no electrolyte<sup>[20]</sup>.

#### H. Anti-microbial activity

The agar spread method was used to determine how effective the ligand and its complexes were against bacteria. We have utilized ram-positive bacteria like

Staphylococcus aureus and Gram-negative bacteria like Escherichia coli (E. coli), with ampicillin as the gold standard antibiotic. The-scale bacterial inhibition was determined. culturing medium was nutrient agar. As a solvent, dimethyl sulfoxide was utilized. As measured by the disc susceptibility test, the total concentration of all chemicals in this solvent was 10.00 mg/ml.

The zone of inhibition is revealed in this method as it pertains to the growth of bacteria in an agar plate. During this time, the dishes were kept at 37 degrees Celsius<sup>[21]</sup> for 24 hours. The data of table (2) supports the conclusion that all compounds have potent antimicrobial properties. The Schiff base ligand's imine moiety is key of its ability to stifle the growth of the bacteria used in the experiment. Disappointing metal complex antibacterial activity It might be because the imine moiety interacts with the metal ion more strongly than the ligand. Since the imine moiety plays a role in suppression, this interaction will dampen its activity<sup>[22]</sup>.



Staph

Fig.(1-a) Antibacterial Staph



Ecoli

Fig.(1-b) Antibacterial Ecoli.

#### I. Frontier molecular orbitals

The ligand molecule's quantum chemical calculations are carried out by Gaussian 09<sup>[23]</sup>. B3LYP/6-311++G(d,p) calculations for the HOMO and LUMO energies. In quantum chemistry, the energy of molecular orbitals (HOMO and LUMO) and other features like these are crucial factors. Furthermore, this helps to explain various different forms of reaction in a conjugated system,

and is employed by the frontier electron density to forecast the most reactive site in  $\pi$ -electron systems [24]. The HOMO-LUMO separation of the conjugated molecules is rather tiny. The major orbitals involved in chemical stability are the highest occupied molecular orbital and the lowest empty molecular orbital. The HOMO state denotes the capacity to give up an electron, whereas the LUMO state, as an electron acceptor, denotes the opposite ability to gain an electron. The energy gap, which is crucial stability of structures [25], is the difference between the HOMO and LUMO orbital and defines the ionization potential (I) and the electron affinity energy (A), respectively:

$$“I=-EHOMO \text{ and } A=-ELUMO” \dots(1)$$

“The electronegativity ( $\chi$ ), global chemical hardness ( $\eta$ ) and electronic chemical potential ( $\mu$ ) using I and A values are expressed as follows, respectively” [26].

$$“\chi=(I+A)/2, \eta=(I-A)/2, \text{ and } \mu=-(I+A)/2” \dots(2)$$

“Global chemical softness (S) and electrophilicity index ( $\omega$ ) values are defined as follows” [27].

$$“S=1/\eta \text{ and } \omega=\mu^2/2\eta” \dots(3)$$

calculated quantum parameters are summarized in Table(4)

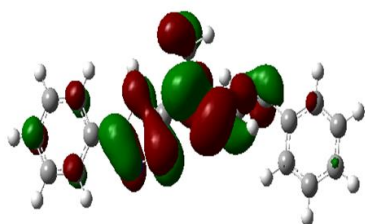


Fig. (2) HOMO orbital

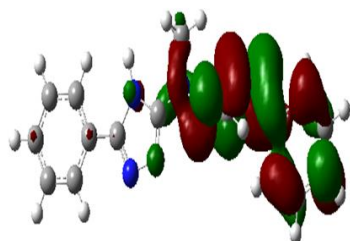


Fig. (3) LUMO orbital

TABLE(2):THEORETICAL GLOBAL REACTIVITY PARAMETERS FOR THE LIGAND

Parameter	Value
HOMO, (eV)	“-7.366”
LUMO, (eV)	“-5.689”
$\Delta E$ , (LUMO-HOMO gap) (eV)	“1.677”
Ionization potential (IP), (eV)	“7.366”
Electron affinity (A), (eV)	“5.689”
Hardness, ( $\eta$ ) (eV)	“0.839”
Softness, (S) (eV) <sup>-1</sup>	“1.192”
Electrophilicity ( $\omega$ ), (eV)	“30.27”
Chemical potential, ( $\mu$ ) (eV)	“-6.528”
Electronegativity, ( $\chi$ ) (eV)	“6.528”

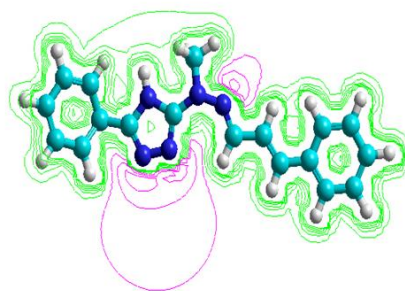


Fig.(4) (a) Graphical presentation of stereochemistry of the Ligand

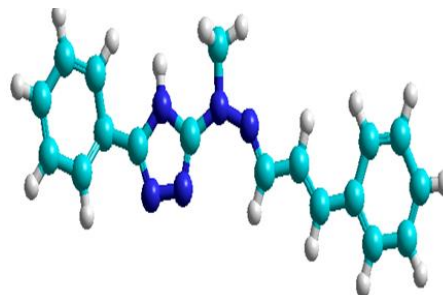


Fig.(b) Electrostatic Potential as 2D Contours for L

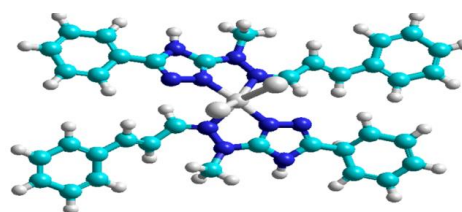


Fig. (5) Graphical presentation of stereochemistry of the complex [Cr(L)<sub>2</sub>Cl<sub>2</sub>]Cl

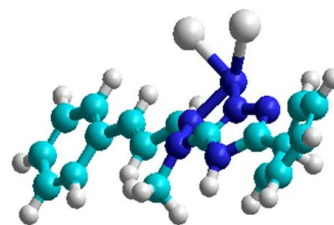


Fig. (6) Graphical presentation of stereochemistry of the complex [Co(L)Cl<sub>2</sub>]

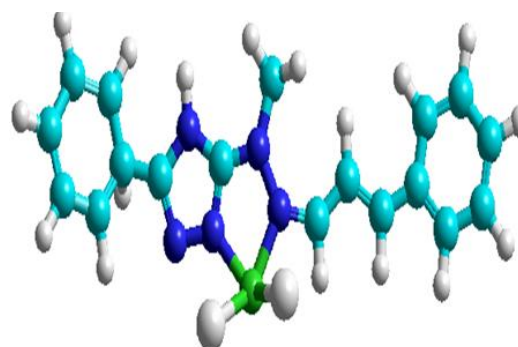


Fig. (7) Graphical presentation of stereochemistry of the complex [Cu(L)Cl<sub>2</sub>]

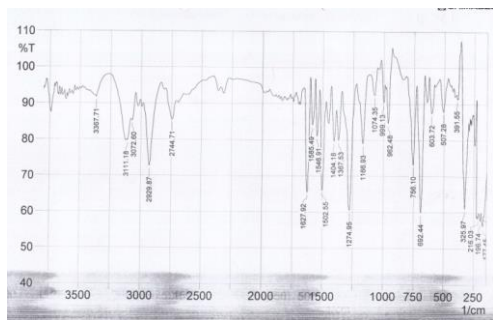


Fig. (8) FT-IR spectrum of the Ligand

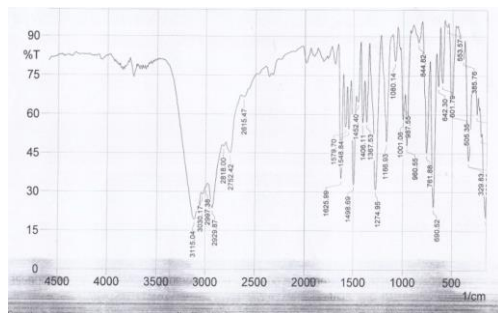


Fig. (9) FT-IR spectrum of the complex  $[Cr(L)_2Cl_2]Cl$

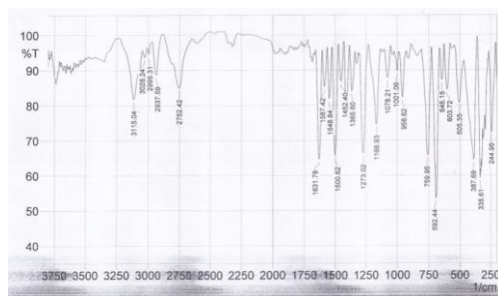


Fig. (10) FT-IR spectrum of the complex  $[Co(L)Cl_2]$

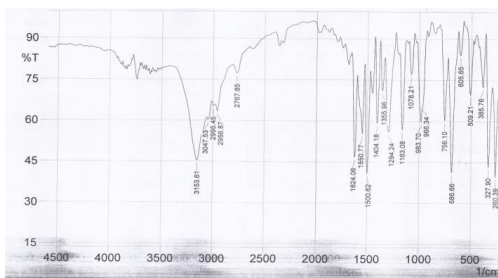


Fig. (11) FT-IR spectrum of the complex  $[Cu(L)Cl_2]$

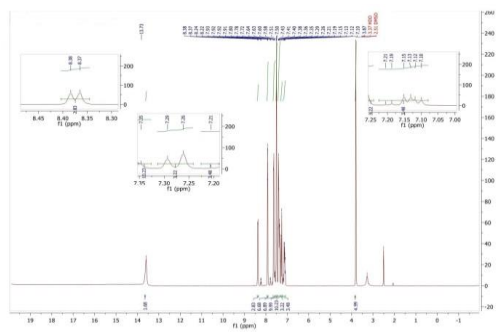


Fig. (12)  $H^1$ -NMR spectrum of the ligand

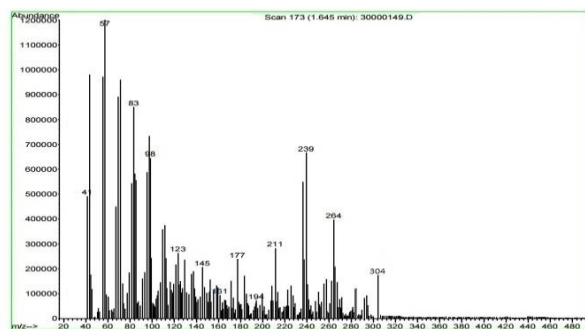


Fig. (13) Mas spectrum of the ligand

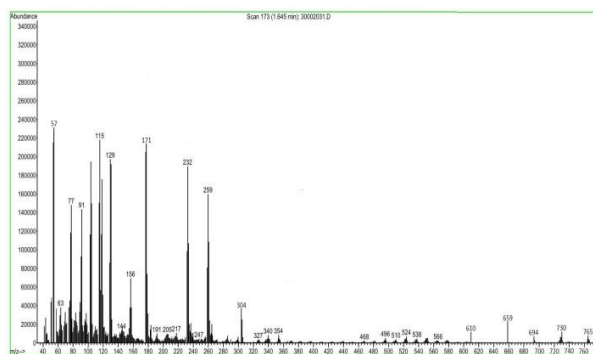


Fig. (14) Mas spectrum of the complex  $[Cr(L)_2Cl_2]Cl$

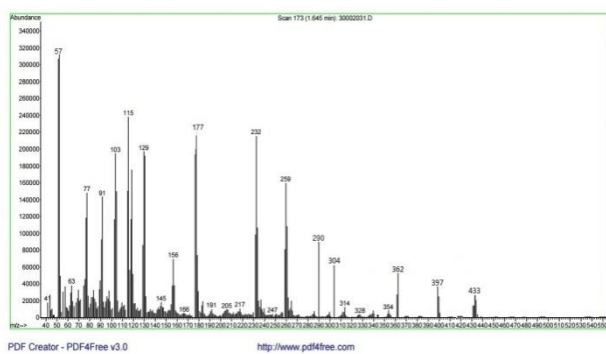


Fig. (15) Mas spectrum of the complex  $[Co(L)Cl_2]$

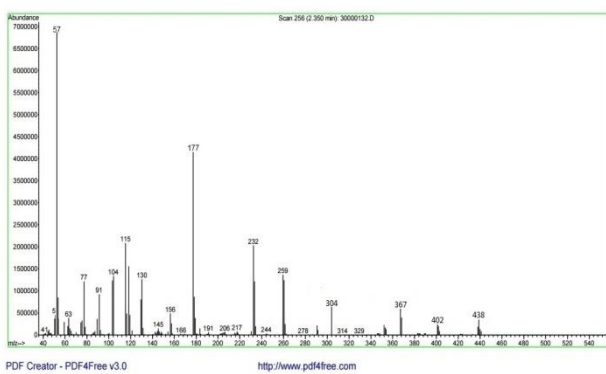


Fig. (16) Mas spectrum of the complex  $[Cu(L)Cl_2]$

“Table (3) Anti-bacterial data of ligand and its complexes”

“No”.	“compound”	E. coli “Inhibition zone” (mm)	Staph. “Inhibition zone” (mm)
“A”	“control”	+++	+++
“B”	L	++	++
“C”	Cr	+	+
“D”	Co	+	+
“E”	Cu	+	+

“+” (6-10) active, “++” (11-15) mm more active, “+++” (16-25) mm highly active

#### IV. CONCLUSION:

This ligand is bivalent in its binding activity. It is clear from the spectroscopic evidence that, NH and the azomethane endo heterocyclic group are involved in coordination with the core transition metal ion. Transition metal complexes have been characterized using a susceptibility magnetic method. A Cr (III) octahedral complex, a Co(II) tetrahedral complex, and a Cu(II) square planer complex are all proposed. Practical results from complexity sites were found to be highly compatible with the findings of the electrostatic potential investigation. It has been shown that the ligand has potent antibacterial properties.

#### REFERENCES

- Nada A. R. & Basim I. Al-A., *J of Global Pharma Tech.*, 10(03):417-430, 2018.
- Timur, I., Kocyigit, U. M., Dastan, T., Sandal, S., Ceribasi, A. O., Taslimi, P. & Ciftci, M., *J Biochem Mol.*, 33(1), 22239, 2018.
- Fayez O. N., Ibrahim A. F. & Saher A. A., *Annals of Tropical Medicine & Public Health*, 24(05), 120-130, 2021.
- Bushra K., Abdullah N., Fareeda A., Shakir A. & Sonu C. T., *J of Biomolecular Structure and Dynamics*, 39(2), 1-51, 2021.
- Paprocka, R., Wiese, M., Eljaszewicz, A., Helmin-Basa, A., Gzella, A., Modzelewska-Banachiewicz, B., & Michal K., *J. Bioorg Med Chem Lett*, 25(13), 2664-2667, 2015.
- El-Sherief, H. A. M., Youssif, B. G. M., Abbas Bukhari, S. N., Abdelazeem, A. H., Abdel-Aziz, M., & Abdel-Rahman, H. M., *Eur J Med Chem.*, 156, 774-789, 2018.
- Shahzad, S. A., Yar, M., Khan, Z. A., Shahzadi, L., Naqvi, S. A. R., Mahmood, A. & Bajda, M., *Bioorg Chem*, 85, 209-220, 2019.
- Sancak K., Ünver Y., Ünlüer D., Düğdü E., G. Kör G., Çelik F. & Birinci E., *Turk. J. Chem.* 36, 457-466, 2012.
- Sancak K., Y. Ünver Y., Kazak C., Düğdü E. & Arslan B., *Turk. J. Chem.* 34, 771-780, 2010.
- Li W., Wu Q., Ye Y., Luo M., Hu L., Gu Y. & Niu F., *Spectrochim. Acta A* 60 (2004) 2343-2354, 2004.
- Ünver Y., Düğdü E., Sancak K., Er M. & Karaoğlu S., *Turk. J. Chem.* 33, 135-147, 2009.
- Youssef N. S. & Hegab K. H., *Synth React Ing Met-Org Nan-Met Chem.*, 35:391-399, 2005.
- Klinge M. H. & Brooker S. *Coord Chem Rev.*, 241(1-2):119-132, 2003.

- Singh D. P., Singh K., Singh Ph. A. & Handa R. N., *J Inst Chemists (India)*, 77, 82, 2005.
- Singh K., Barwa M. S. & Tyagi P., *Eur J Med Chem.*, 41, 147-153, 2006.
- Yildiz M., Dulger B., Koyuncu S. Y. & Yapici B. M., *J Ind Chem Soc.*, 81, 7-12, 2004.
- Chohan Z. H., Hassan M. U., Khan K. M., Supuran C. T., *J Enz Inhib Med Chem.*, 20(2):183-188, 2005.
- Nazarbahjat N., Ariffin A., Abdullah Z., Abdulla M. A., Shia J. K. S. & Leong K. H., *Med. Chem. Res.*, 25(9), 2015-2029, 2016.
- Gary D. A. T. & Miessler L., “Inorganic chemistry.” pearson prentice hall, 1991.
- Khalid J. AL-A., Ahmed K. A. & Ali M. T., *J of Mole Stru.*, 1108, 378-397, 2016.
- Ahmad I. & A. Z. Beg A. Z., *Ethnopharmacology J.*, 74(2), 113-123, 2001.
- Riyadh M. A., Enaam I. Y. & Mohamad J. Al-J., *The Scientific World J.*, 2013, 1-6, 2013.
- Jesby G., Sajan D, Javeesh A., Arun A., Vinita G., Chitra R., *Optics and Laser Tech.*, 105 207-220, 2018.
- Choi, C. & Kertez, M., *J. Phys. Chem.* 101A, 3823-3831, 1997.
- Mokhtaria D., Nadia B., Youcef M., Rahmani R., Abdelkader C. and Fodil H., *Molecules*, 20, 4042-4054, 2015.
- Mendoza-Huizar L. H., *J. Mex. Chem. Soc.* 58(4), 416-423, 2014.
- Ustabas R., Süleymanoglu N., Ünver Y. & Direkel S., *J of Molecular Structure.*, 1214, 2-8, 2020.
- Hout R., Pietro W. J. & Herhre W. J., John Wiley, New York, 1, (1984).